Journal of Hydrology 567 (2018) 382–392

Contents lists available at ScienceDirect

Journal of Hydrology

journal homepage: www.elsevier.com/locate/jhydrol

Research papers

Quantifying the impacts of small dam construction on hydrological alterations in the Jiulong River basin of Southeast China

Weiwei Lu, Huimin Lei, Dawen Yang*, Lihua Tang, Qinghua Miao

State Key Laboratory of Hydroscience and Engineering, Department of Hydraulic Engineering, Tsinghua University, Beijing 100084, China

ARTICLE INFO

This manuscript was handled by G. Syme, Editor-in-Chief, with the assistance of Bellie Sivakumar, Associate Editor

Keywords:
Flow regime
Indicators of hydrological alterations
Distributed hydrological model
Post bias correction method
Small dam construction

ABSTRACT

The hydrological alterations induced by dam construction modify natural flora and fauna habitats and impair ecosystem stability. Although many studies have documented the impacts of large dams on streamflow, few have described the effects of small dam construction on hydrological conditions. The cumulative effects of intensive small dams may also cause severe ecological problems. To evaluate the impacts of dam construction on the indicators of hydrological alterations, a framework that combined a hydrological model and the post bias correction method was proposed. The hydrological alterations of two individual rivers in the Jiulong River basin that experienced impacts from intensifying small hydropower reservoirs, the North River and the West River, were analyzed using the proposed framework. The results show that the framework can successfully avoid misleading the impacts of dam construction on monthly runoff and multi-minimum values detected by the previously common method that did not separate the impacts of climate change and dam construction on flow regime. The small hydropower-dominated North River and the flood-control-dominated West River exhibited generally consistent change patterns of unchanging monthly river discharge, reduced high pulse count, reduced rise and fall rates, and increased number of reversals. Conversely, the changes to several Indicators of Hydrologic Alterations (IHA) differed between the two rivers. The flood-control-dominated West River exhibited 1) increased indicators, such as the base flow index, multi-day minimum flow and high pulse duration and 2) decreased multi-day maximum flow and low pulse count. Unlike the West River, the hydropower-dominated North River experienced 1) increased low pulse count and 2) decreased indicators such as multi-day minimum flow and low pulse duration. Our results implied that the ecological impacts of the small hydropower-dominated North River may exceed those of the flood-control-dominated West River. Therefore, the minimum ecological water demand should be considered not only in the large reservoirs operation, but also in the operation of small hydropower reservoirs.

1. Introduction

Dam construction has substantially altered the flow regimes of the majority of the rivers throughout the world (Naiman et al., 1993). The construction of dams can alter the natural flow regime by affecting the magnitude, frequency, duration, timing, and rate of change in the flow (Richter et al., 1996; Nislow et al., 2002; Magilligan and Nislow, 2005) as well as by changing the sediment, nutrients, energy and biota (Ligon et al., 1995). Changes in flow regimes within the context of dam construction result in extensive environmental degradation and loss of biological diversity (Lytle and Poff, 2004; Ziv et al., 2012; Castello and Macedo, 2016). Therefore, it is necessary to assess the degree of deviation from the natural flow regime characteristics that is induced by dam construction to provide support for the maintenance of fundamental ecological functions (Arthington et al., 2006; Poff et al., 2010; Schneider et al., 2013). In this regard, over 170 metrics have been developed to describe the different characteristics of the flow regime, among which the indicators of hydrologic alterations (IHA) method (Richter et al., 1996) has been widely used (Olden and Poff, 2003; Gao et al., 2009).

Highly regulated rivers in China are dominated by large-scale ecosystem alterations induced by hydrological alterations. Many of the previous studies associated with dam-induced hydrological alterations across river basins in China have focused on the impacts of large dams that generally aim to control floods in large basins, such as the Lancang River (Zhao et al., 2012), the Mekong River (Li et al., 2017), the Pearl River (Zhang et al., 2014), the Yangtze River (Gao et al., 2012) and the Yellow River (Yang et al., 2012; Zhang et al., 2018). All of these studies

* Corresponding author.
E-mail address: yangdw@tsinghua.edu.cn (D. Yang).

https://doi.org/10.1016/j.jhydrol.2018.10.034
Received 31 May 2018; Received in revised form 13 October 2018; Accepted 15 October 2018
Available online 18 October 2018
0022-1694/ © 2018 Elsevier B.V. All rights reserved.

used the IHA method to evaluate the hydrological impacts of dam construction. In general, these studies found that the operation of large dams (1) reduced the streamflow during wet seasons and increased the streamflow during dry seasons, (2) reduced the maximum flow values, and (3) increased the number of reversals but decreased the rates of rise and fall. However, the minimum flow values, base flow indexes and pulsing behaviors varied depending on the operation, size and location of the dam, i.e., increases in the Yangtze and Mekong River (Li et al., 2017; Gao et al., 2012; Magilligan and Nislow, 2005) and decreases at several stations in the Yellow River (Zhang et al., 2018). These hydrological alterations caused further environmental problems. For example, the Three Gorges Dam in the Yangtze River caused reduced flow pulses that led to diminished aquatic biodiversity and fish populations (Gao et al., 2012). Moreover, the magnitudes of large floods decreased, and the high flow variability decreased the connectivity between the floodplain and the river channel, which may have further reduced the species richness and abundance of waterfowl and aquatic plants (Wang et al., 2016a,b). Large decreases in the magnitude of high flow due to damming in the Mekong River caused the trapping of sediments, which altered the nutrient dynamics and other biogeochemical processes in the related deltas, estuaries, and marine-shelf ecosystems (Kondolf et al., 2014; Li et al., 2017).

In addition to large dams, the development of small dams has also been highlighted in national energy policies in China (Li and Ma, 2009). Therefore, small dam construction is intense in China, especially in South China where the hydropower resources are extensive. Small dams are mainly designed for hydropower generation and may be constructed anywhere in the catchment where appropriate physical conditions exist (Deitch et al., 2013). Although small dams may not be individually capable of significantly influencing the streamflow, the cumulative effects of many small dams may exceed those of large hydropower dams, particularly with regard to ecologically relevant flow regimes (Deitch et al., 2013; Kibler and Tullos, 2013). However, analogous research addressing the effects of high-density small dams on hydrological conditions are scarce.

We thus present an investigation of the hydrological impacts of intense small hydropower development in the Jiulong River basin, which is a typical small catchment in southeast China. To this end, a framework for evaluating the impacts of dam construction on the flow regime was first proposed, and then the changes in the flow regime before and after dam construction were analyzed by using this framework.

2. Study area and data acquisition

2.1. The Jiulong River basin

The Jiulong River basin is a subtropical coastal watershed in southeast China with a drainage area of 14,741 km^2 (Fig. 1). The mean annual runoff is 1010 mm and the annual precipitation ranges from 1400 mm to 1800 mm and nearly 75% of the precipitation occurs from April to September. The mean annual temperature is 19.9–21.1 °C. Two major tributaries, the North River and West River, cover nearly 95% of the total area of the Jiulong River basin. The basin had 193 constructed reservoirs with storage capacities of $\sim 1.11 \times 10^9$ m^3 by the end of 2011, which were built for flood control, hydropower generation, irrigation and domestic and industrial water use.

2.2. Data acquisition and processing

Three hydrological stations and 10 meteorological stations in the Jiulong River basin are available within the study area (Fig. 1). The daily river discharge data were obtained from the Hydrology and Water Resources Bureau. The meteorological data, including daily air temperature (mean, maxima and minima), daily relative humidity, daily sunshine duration and daily wind speed, were obtained from the national meteorological stations managed by the China Meteorological Administration (CMA). Precipitation data were from the 0.25° × 0.25° China Gauge-based Daily Precipitation (CGDPA) Product (Shen et al., 2014). The meteorological data were first interpolated to grids using an angular distance weighting method since the meteorological stations are sparse and unevenly distributed in the study area (New et al., 2000), and the 0.25° × 0.25° precipitation data were resampled to a 1-km grid using the nearest neighbor assignment in ArcGIS Software. After spatial interpolation, the duration of the rainfall in a day was determined by the daily rainfall amounts (the more rain, the longer the duration) (Gao et al., 2016). The precipitation start time in a day is determined randomly, and the daily precipitation amounts were downscaled into hourly precipitation by a normal distribution (Gao et al., 2016).

The land cover data (at a 30 m resolution) in 2000 were from the Geographical Information Monitoring Cloud Platform (http://www.dsac.cn/). The land cover map was been reclassed into 10 categories, including water body, urban area, bare soil, forest, irrigated cropland, upland, grassland, shrub, wetland, and ice. For each land use type, a 15-day leaf area index (LAI) was calculated by the normalized difference vegetation index (NDVI) values (Sellers, 1996). The NDVI data with 15-day and 0.05° × 0.05° temporal and spatial resolutions from 1982 to 2014 were collected from the 3rd generation of NDVI (NDVI3g) from Global Inventory Modeling and Mapping Studies (GIMMS) data. The NDVI input in the geomorphology-based hydrological model (GBHM) before 1982 was replaced by the NDVI data in 1982 (Ma et al., 2010). The soil hydraulic parameters, including saturated soil moisture, residual soil moisture and soil hydraulic conductivity and parameters α and n in the van Genuchten model were provided by the China Soil Hydraulic Parameters Dataset, which was provided by Dai et al. (2013). Digital elevation data with a resolution of 90 m were downloaded from the shuttle radar topography mission (SRTM) database (Jarvis et al., 2008). The reservoir information achieved from a water resource planning survey implemented in 2011 included the reservoir name, year of completion, controlled basin area, reservoir capacity and reservoir function.

3. Methodology

3.1. Indicators of hydrologic alterations

The IHA method was first proposed by Richter et al. (1996) to evaluate the hydrological regime changes induced by various human activities, such as dam operations, flow diversion, or groundwater pumping. The IHA method includes 33 biologically relevant hydrological parameters that characterize the intra-annual variations in streamflow conditions. Richter et al. (1996) proposed the 33 IHA parameters because of high sensitivity of physical habitat alteration in lotic systems and high frequency of occurrences in limnology studies. The 33 hydrological indicators are generally divided into the following 5 groups: 1) the magnitude of the monthly discharge, 2) the magnitude and duration of the annual extreme streamflow, 3) the timing of the annual extreme streamflow, 4) the frequency and duration of high and low pulses, and 5) the rate and frequency of flow changes (Table S1). Because no zero flow events occurred in this region, 32 hydrological indicators (excluding zero flow days) were applied in this study.

3.2. A framework for evaluating the impacts of dam construction on flow regime

A previously common method to assess the hydrological impacts of dam construction using IHA methods divided the pre-impact and post-impact period and then calculated the relative change between the observed IHA metrics during the pre-impact period and post-impact period (Gao et al., 2012; Yang et al., 2012). The previously common method requires less data and easier to be accomplished. However, the method that relies on observed flow data ignores the impacts of climate

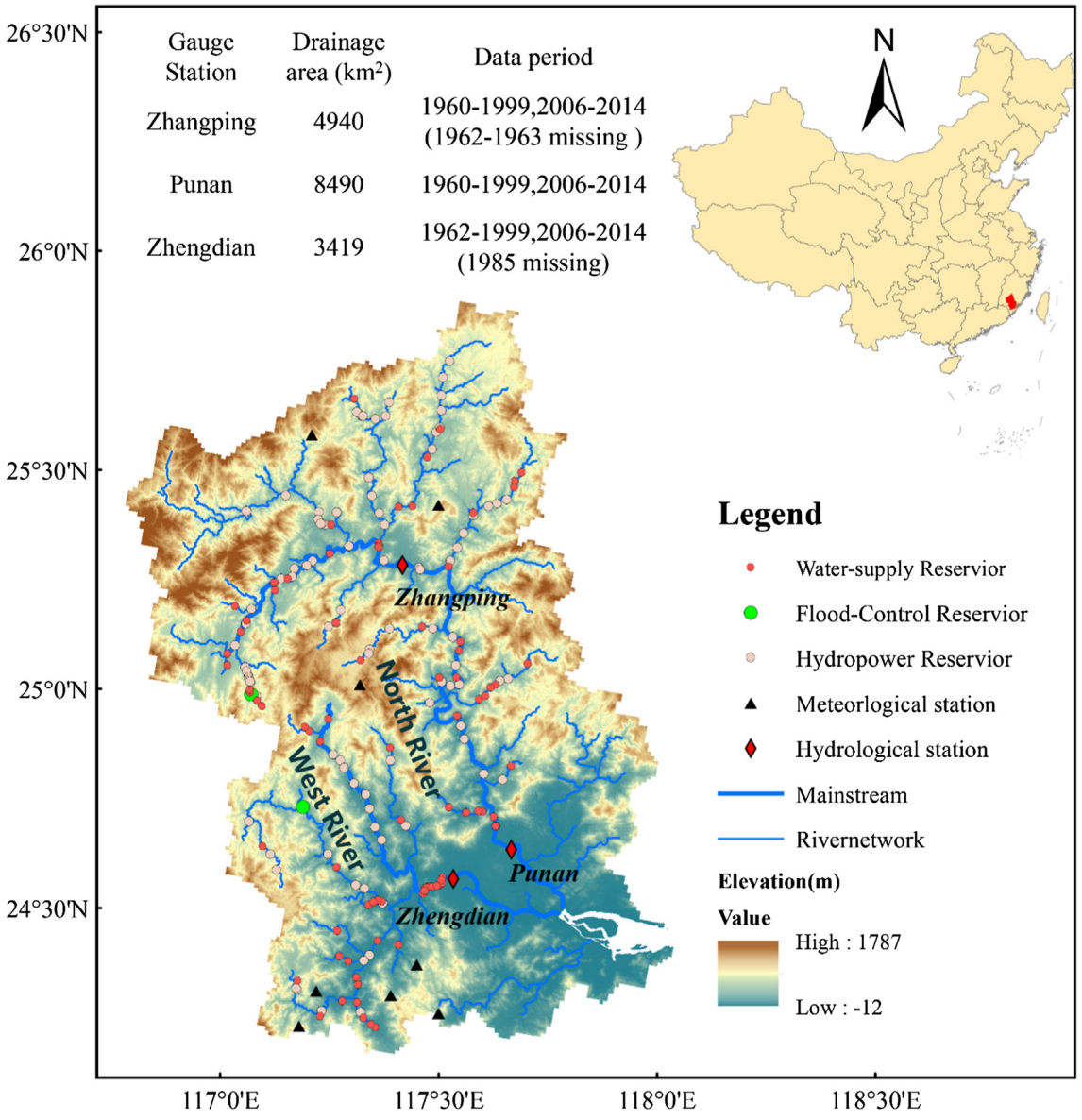

Fig. 1. Map of the Jiulong River Basin, illustrating the distribution of existing reservoirs and observation stations used in this study.

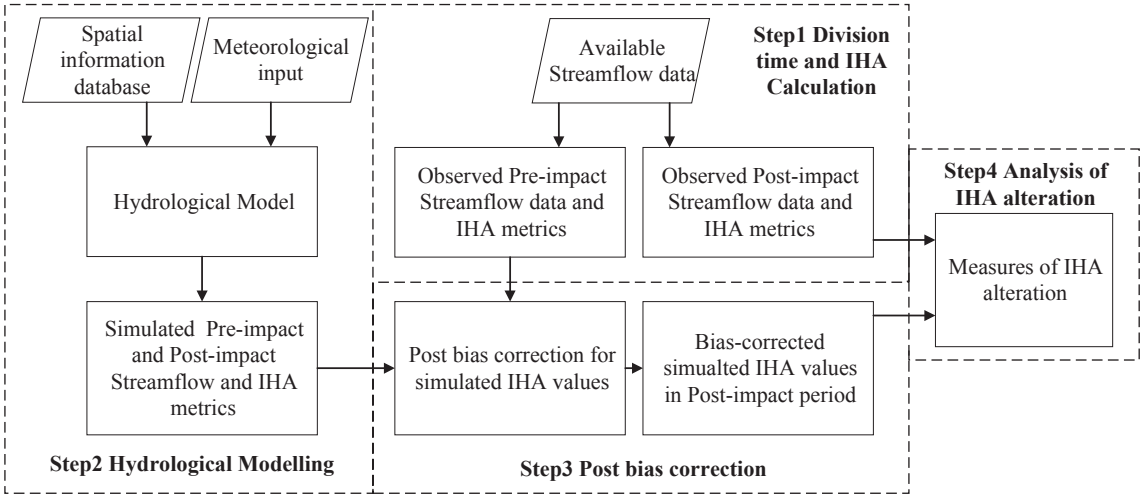
Spatial information database
Meteorological input
Hydrological Model
Simulated Pre-impact and Post-impact Streamflow and IHA metrics
Step2 Hydrological Modelling
Available Streamflow data
Step1 Division time and IHA Calculation
Observed Pre-impact Streamflow data and IHA metrics
Observed Post-impact Streamflow data and IHA metrics
Post bias correction for simulated IHA values
Bias-corrected simualted IHA values in Post-impact period
Step3 Post bias correction
Step4 Analysis of IHA alteration
Measures of IHA alteration

Fig. 2. Framework for evaluating the impacts of dam construction on flow regime.

Table 1
The parameters used in GBHM.

Category	Parameters	Estimating method
Land surface and vegetation parameters	Leaf area index (LAI)	Estimated from GIMMS NDVI (Sellers, 1996)
	Surface retention capacity	Estimated for each land use type according to the soil-water conservation practice
	Surface Manning roughness coefficient	
	Soil anisotropy ratio	
Soil water parameters	Saturated volumetric moisture content	Obtained from China Dataset of soil Properties for Land Surface Modeling
	Residual volumetric moisture content	
	Saturated hydraulic conductivity at surface	
	Parameter for soil water retention curve and hydraulic conductivity in van Genuchten's (1980) equation	
Channel parameters	River geometry	Estimated for river sections using the hydrological station measurement
Others	River Manning roughness coefficient	Refer to Maidment et al. (1993)
	Hydraulic conductivity of groundwater	From calibration
	Groundwater storage coefficient	From calibration
	Saturated hydraulic conductivity at the bottom	From calibration
	Slope shape factor	From calibration

change and ascribes the observed hydrological alteration to the impacts of dam construction. Climate change maybe alter hydrological regimes greatly (Magilligan and Nislow, 2005; Timpe and Kaplan, 2017). Therefore, a new framework was proposed to eliminate the impacts of climate change when quantifying the hydrological impacts of dam construction. Since post-impact flow regime simulated by hydrological model without dam regulation module represented the natural flow regime and observed post-impact flow regime represented the altered flow regime influenced by climate change and dam construction, the framework quantified the impacts of dam construction through subtracting the simulated post-impact flow regime from the observed flow regime. The framework consists of four main steps (Fig. 2). (1) The Pettitt test (Pettitt, 1979) was used to identify the abrupt change point of the reservoir capacities variations during the available streamflow period and the whole period was divided into a pre-impact and post-impact period based on the abrupt change point; then the observed IHA metrics for the two periods were calculated. (2) A distributed GBHM was employed to simulate the natural flow series during the post-impact period. (3) Based on the observed and simulated pre-impact IHA metrics, post bias correction was used to obtain bias-corrected simulated IHA values in the post-impact period. (4) The observed and bias-corrected simulated post-impact flow statistics were compared to estimate the flow alteration due to dam construction.

3.2.1. *Brief description of the distributed hydrological model and evaluation*

In this study, the daily runoff in the Jiulong River basin, a humid catchment over the period from 1960 to 2014 need to be simulated by a hydrological model. The GBHM developed by Yang et al. (1998, 2002) has been successfully applied in humid regions like Yangtze River (Li et al., 2015), Mekong River (Wang et al., 2016a,b) and Chao Phraya River (Yang and Musiake, 2003) and performs well in simulating daily runoff. Therefore, the GBHM is used in this study to simulate the natural streamflow processes over the period from 1960 to 2014. The distributed model is forced by meteorological data, and the regulations of dams are not included in the model structure.

The GBHM uses a basin subdivision scheme and a sub-grid parameterization scheme. The Horton-Strahler scheme is applied to subdivide the study basin into subcatchments and order the river network conveniently based on the DEM data. Each subcatchment is divided into several flow intervals according to the flow distance to the outlet, and then a flow interval is generalized as a series of hillslope units. The hillslope unit is the computational unit for hydrological simulation (Yang et al., 2002, 2004). Hydrological simulation in the GBHM includes two main components: the hillslope hydrological module and flow routing module (Yang et al., 2004). The hydrological processes calculated in the hillslope hydrological module are canopy interception, evapotranspiration, infiltration, surface flow, subsurface flow, and exchange between groundwater and the river. The flow routing in the river network was solved using the kinematic wave approach. More information about methods used in these hydrological processes in GBHM can be found in Yang et al. (2002, 2004).

In the present study, the GBHM uses a 1-km resolution hillslope and is implemented on a one-hour time step. A warm-up run of the model from 1960 to 1962 was used to get a stable value of model state variables such as soil moisture, groundwater table and river water depth at the beginning of 1963. Specifically, the model ran recursively during 1960–1962 and the nse and bias were calculated using simulated streamflow from the latest run and the last run. If nse is equal to 1 and bias ranges from −0.3% and 0.3%, the warm-up run can be stopped and the stable value of model state variables at the beginning of 1963 was obtained. After the warm-up run, the daily river discharge data from 1963 to 1967 were used to calibrate the model parameters. The objective of calibration is to constrain the percent bias (PBIAS) between −10% and 10%, and constrain the Nash and Sutcliffe efficiency (NSE) coefficient and logarithmic-transformed Nash and Sutcliffe efficiency (LNSE) coefficient to > 0.7 according to the general performance recommended by Moriasi et al. (2007). The parameters used in the GBHM are listed in Table 1 (Miao et al., 2016). The manually calibrated parameters in the GBHM included the hydraulic conductivity of groundwater, groundwater storage coefficient, slope shape factor and saturated hydraulic conductivity at the bottom.

The daily river discharge from 1968 to 1972 was used for model validation, and then simulations were performed from 1963 to 2014. The NSE (Nash and Sutcliffe, 1970), LNSE (Smakhtin et al., 1998) and PBIAS (Gupta et al., 1999) were adopted to evaluate the model performance in terms of the accuracy of simulated daily data compared to the measured daily flow, which are defined as

$$NSE = 1-\frac{\sum_{t=1}^{T}(Q_{sim}^{t}-Q_{sim}^{t})^2}{\sum_{t=1}^{T}(Q_{obs}^{t}-\bar{Q}_{obs})^2} \quad (1)$$

$$LNSE = 1-\frac{\sum_{t=1}^{T}(ln(Q_{sim}^{t})-ln(Q_{sim}^{t}))^2}{\sum_{t=1}^{T}(ln(Q_{obs}^{t})-ln(\bar{Q}_{obs}))^2} \quad (2)$$

$$PBIAS = \frac{\sum_{t=1}^{T}(Q_{obs}^{t}-Q_{sim}^{t})\times 100}{\sum_{t=1}^{T}Q_{obs}^{t}} \quad (3)$$

where $Q_{obs}^{t}$and $Q_{sim}^{t}$are the observed and simulated streamflow at time t, respectively, $\bar{Q}_{obs}$is the average value of the observed streamflow during the period T.

To evaluate the ability of a hydrological model to replicate IHA values, two statistical methods were employed: (1) Pearson correlation

coefficient and (2) Mann-Whitney *U* test (Nachar, 2008). The correlation analysis evaluated the simulation accuracy of the interannual variabilities of those IHA values, while the Mann-Whitney *U* test examined the statistical significance of the mean differences between the observed and simulated IHA values.

According to the recommendation by Moriasi et al. (2007), NSE/LNSE values between 0.65 and 1.0 and PBIAS values between -10% and 10% indicate that the model performs well at simulating the daily discharge process. In this study, the IHA value passes the Mann-Whitney *U* test, which means that the observed and simulated mean values are not significantly different, and the Pearson correlation coefficient is higher than 0.4, which represents that the model can adequately replicate the corresponding IHA values (Shrestha et al., 2014; Ryo et al., 2015).

3.2.2. Post bias correction for the simulated IHA values

The objective function for manual calibration of the model is single and the model is calibrated step by step. Firstly evaporation-related parameters are adjusted to reduce PBIAS value within the reasonable range defined in the study. Then other parameters such as the hydraulic conductivity of groundwater, groundwater storage coefficient, slope shape factor and saturated hydraulic conductivity at the bottom are adjusted to make NSE and LNSE values reach the expected level and maintain PBIAS value within the recommended range. Because our calibration objective is to maintain PBIAS, NSE and LNSE in a recommended range, this cannot guarantee that each IHA metric is appropriately simulated. However, quantification of the impacts of dams requires a relatively high model accuracy when reproducing the IHA values; thus, it is necessary to remove the possible bias from the simulated mean IHA values. To this end, a simple bias removal method called the quantile mapping method (Panofsky and Brier, 1968) was used in this study. This method removes the mean bias by matching the cumulative distribution functions (CDF) of the observed and simulated IHA values. The quantile mapping method has the benefit of accounting for biases in all statistical moments, and it is assumed that biases relative to observations at each quantile are constant during the projections (Thrasher et al., 2012). There are three major limitations of this method (Boé et al., 2007): i) the temporal autocorrelation properties of the series are not corrected; ii) each variable is corrected independently; iii) the spatial autocorrelation of the different variables may be biased. This approach has been used extensively to reduce the bias of satellite retrievals of soil moisture (Reichle and Koster, 2004) and correct the systematic distributional bias in precipitation and temperature outputs from climate models (Piani et al., 2010). In particular, Hashino et al. (2007) used the quantile mapping method to shift the probability distribution of the ensemble forecasts of monthly streamflow.

Fig. 3 shows the principal scheme of the quantile mapping method. Taking one IHA value as an example, the observed and simulated CDF in the pre-impact period and the simulated CDF in the post-impact period can be obtained through empirical quantiles of data (i.e., the sorted values in a sample). The steps that obtain corrected CDF for simulated CDF in the post-impact period are as follows:

Step1: x_{sim} reprensents the simulated value smaller than the largest simulated value in the pre-impact period max_{sim} on simulated CDF in the post-impact period. Probabilities p_1 and p_2 corresponding to x_{sim} can be found for the simulated CDF during the pre-impact period and post-impact period, respectively;
Step2: Given the probability p_1, the value x_{corr} can be obtained from the observed CDF during the pre-impact period;
Step3: (p_2, x_{corr}) on corrected CDF is the corrected point of (p_2, x_{sim}) on simulated CDF in the post-impact period;
Step4: y_{sim} reprensents the simulated value larger than max_{sim}. The largest observed value max_{obs} in the pre-impact period and probabilities p_3 corresponding to y_{sim} for the simulated CDF during post-impact period can be obtained;
Step5: (p_3, $y_{sim} + max_{obs} - max_{sim}$) on corrected CDF is the corrected point of (p_3, y_{sim}) on simulated CDF in the post-impact period.

4. Results

4.1. Model performance in simulating streamflow and IHA metrics

Fig. 4 shows the observed and simulated daily logarithmic-transformed river discharge at the Zhangping (upper North River), Punan (lower North River) and Zhengdian (lower West River) stations during the calibration period (1963–1967) and validation period (1968–1972). The PBIAS, NSE and LNSE values for the simulated daily discharges at the three stations are listed in Table 2. The simulated river discharge at the Zhangping (upper North River) station and Punan (lower North River) station exhibited similar results with PBIAS values greater than −9% and NSE/LNSE values larger than 0.79, which indicated that the daily discharge simulations in the North River were very good. Although the statistics at the Zhengdian (lower West River) station were slightly worse than those in the North River, the simulation discharge at the Zhengdian (lower West River) station still performed well. In general, the model effectively captured the temporal variability of streamflow at all three stations.

Table 3 depicts the Pearson correlation coefficient and results of the Mann-Whitney *U* test between the observed and GBHM-simulated IHA values for the three stations during the pre-impact period. The number in bold means that the observed and GBHM-simulated IHA values were significant differences at the 95% confidence level. Fig. S1 shows the

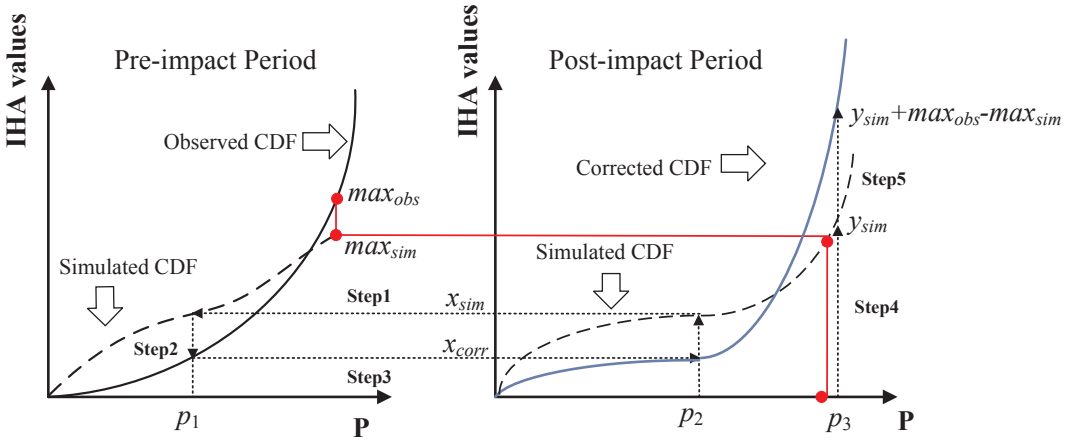

Fig. 3. Principle scheme of the quantile mapping method.

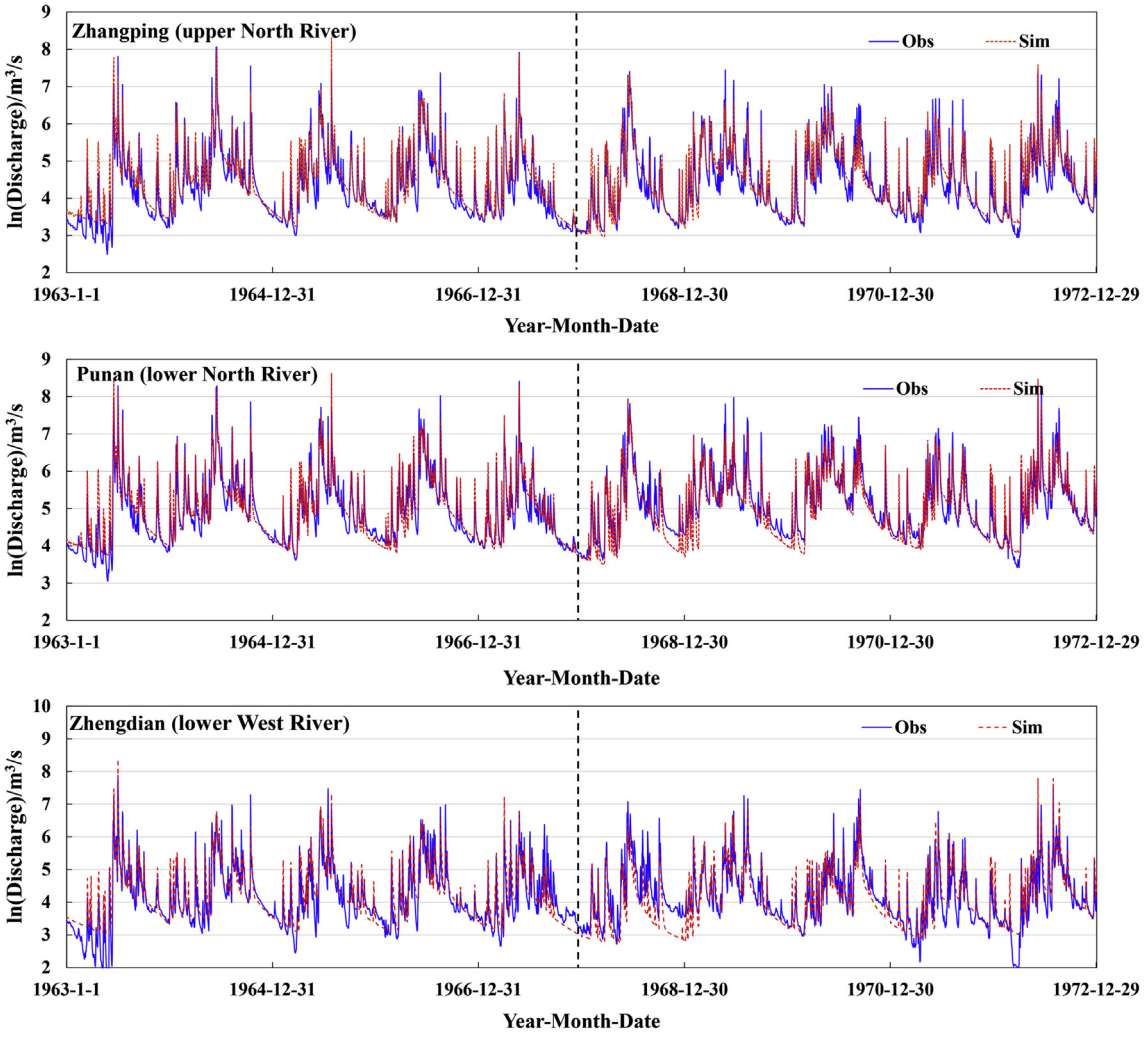

Fig. 4. Comparisons of simulated (Sim) and observed (Obs) daily logarithmic transformed streamflow at Zhangping (upper North River), Punan (lower North River) and Zhengdian (lower West River) stations during the calibration period (1963–1967) and validation period (1968–1972).

observed and simulated 30-day minimum and 1-day maximum value at three stations from 1963 to 2014. Of the 32 IHA values, 29 for Zhangping (upper North River) station, 29 for Punan (lower North River) station and 24 for Zhengdian (lower West River) station passed the Mann-Whitney *U* test and had Pearson correlation coefficients greater than 0.4, representing that the model can adequately replicate the corresponding IHA value when simulating most of the IHA values at the three stations. However, the fall rate, number of reversals at three stations and low-flow related IHA indicators, such as 1-day, 3-day, 7-day, baseflow index, low pulse count and duration at the Zhengdian (lower West River) station, showed significant differences in mean values but relatively high correlation values (> 0.4). In addition, low pulse duration at the Zhangping (upper North River) station and rise rate at the Punan (lower North River) station have low correlation values but no significant difference in mean values.

4.2. Changes in reservoir storage

Fig. 5 shows the accumulated water storage capacities in the drainage area of Zhangping (upper North River), Punan (lower North River), and Zhengdian (lower West River) stations in the Jiulong River basin from 1956 to 2011. Based on the Pettitt test (Pettitt, 1979), the abrupt change point was 1973 for the West River station, whereas it was 1976 for the North River stations at a significance level of 0.05. The extracted change points represented the start year of intensive dam construction. Therefore, for the North River stations, the streamflow from 1963 to 1999 and 2006–2014 were separated into a pre-impact period (1963–1975) and a post-impact period (1976–1999, 2006–2014); for the West River station, the pre-impact period was 1963–1972, and the post-impact period was 1973–1999 and 2006–2014.

Table 2
GBHM performance for daily discharge simulation.

Gauge Station	Calibration period (1963–1967)			Validation period (1968–1972)		
	PBIAS (%)	*NSE*	*LNSE*	PBIAS (%)	*NSE*	*LNSE*
Zhangping (upper North River)	8.91	0.79	0.86	2.11	0.79	0.87
Punan (lower North River)	3.77	0.82	0.90	-8.77	0.85	0.86
Zhengdian (lower West River)	4.70	0.72	0.80	-8.00	0.69	0.74

Table 3
Pearson correlation coefficient and Mann-Whitney *U* test results for the observed and simulated IHA metrics during pre-impact period at Zhangping (upper North River), Punan (lower North River) and Zhengdian (lower West River) stations.

IHA metrics	Pre-impact period (1963–1975) Zhangping (upper North River) Correlation coefficient	Pre-impact period (1963–1975) Punan (lower North River) Correlation coefficient	Pre-impact period (1963–1972) Zhengdian(lower West River) Correlation coefficient
January	0.98	0.97	0.92
February	0.95	0.94	0.91
March	0.99	0.99	0.95
April	0.98	0.99	0.96
May	1.00	0.99	0.96
June	0.94	0.91	0.68
July	0.84	0.92	0.94
August	0.94	0.93	0.80
September	0.90	0.95	0.96
October	0.91	0.88	0.88
November	0.95	0.94	0.92
December	0.94	0.93	0.84
1-day min	0.78	0.68	**0.68**
3-day min	0.81	0.71	**0.69**
7-day min	0.87	0.79	**0.81**
30-day min	0.97	0.91	0.90
90-day min	0.97	0.97	0.88
1-day max	0.58	0.62	0.69
3-day max	0.77	0.76	0.84
7-day max	0.91	0.92	0.74
30-day max	0.95	0.94	0.73
90-day max	0.98	0.95	0.67
Base flow index	0.61	0.58	**0.55**
Date of max	0.89	0.71	0.60
Date of min	0.46	0.58	−0.20
Low pulse count	0.72	0.79	**0.66**
Low pulse duration	0.19	0.48	**0.64**
High pulse count	0.57	0.69	0.79
High pulse duration	0.83	0.69	0.85
Rise rate	0.69	0.30	0.19
Fall rate	**0.84**	**0.84**	**0.60**
Number of reversals	**0.59**	**0.47**	**0.41**

Note: The number in bold means the parameter is significant at 95% confidence level using Mann-Whitney *U* test (Nachar, 2008).

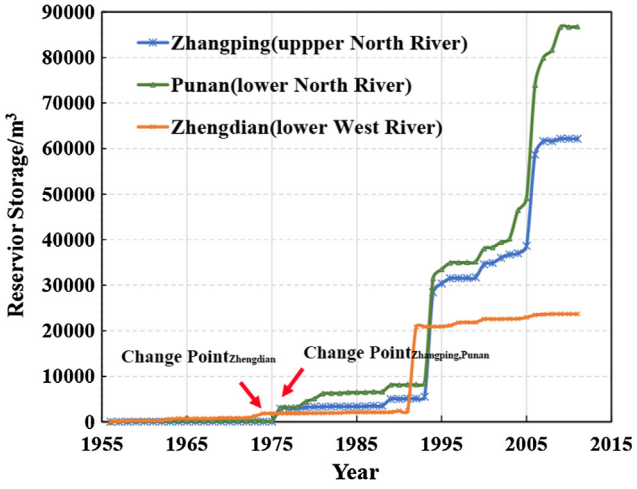

Fig. 5. The accumulated water storage capacities in the drainage areas of Zhangping (upper North River), Punan (lower North River) and Zhengdian (lower West River) stations in Jiulong River basin during 1956–2011.

The 193 reservoirs constructed in the Jiulong River basin were built to meet certain purposes, such as flood control, hydropower generation, and water supply (including irrigation, domestic and industrial water use). A total of 51% of these reservoirs are single-purpose reservoirs, of which 98% serve for hydropower generation. The rest are multipurpose reservoirs that serve several purposes with different precedence levels. The higher precedence level of one purpose of one multipurpose reservoir means that the purpose should be satisfied first when it conflicts with other purposes with lower precedence levels. For simplicity, we assumed that the operation rules of multipurpose reservoirs are determined by the purpose with the highest precedence level.

Fig. 1 shows the distribution of the existing reservoirs used in this study. All of the reservoirs are widely spread throughout the Jiulong River basin, and 135 out of the 193 reservoirs are located in tributaries. Hydropower reservoirs accounted for 68% and 60% of the reservoirs in the drainage areas of the Zhangping (Upper North River) station and Punan (lower North River) station, respectively, while 41% of the reservoirs are hydropower reservoirs in the drainage area of the Zhengdian (lower West River) station. Only two flood-control reservoirs exist in the Jiulong River basin, and both are located in the tributaries.

The reservoir capacities for hydropower, flood control and water supply in the drainage areas of three stations in the Jiulong River basin by the end of 2011 are shown in Fig. 6. The reservoirs in the drainage areas of the Zhangping and Punan (North River) stations had largest hydropower storage capacities, while those in the drainage area of the Zhengdian (lower West River) station had largest flood-control storage capacities. In the drainage areas of the Punan and Zhangping (North River) stations, the hydropower reservoir storage is far greater than the storage of the other two reservoir types. In the drainage area of the Zhengdian (lower West River) station, water supply reservoirs are most abundant, but they have the smallest storage capacities, and the flood-control reservoir has the largest storage capacity. Hence, the streamflow at the Zhangping and Punan (North River) stations are dominantly affected by hydropower reservoirs, and that at the Zhengdian (lower West River) station is mainly influenced by flood-control reservoirs.

4.3. Impact of dam construction on flow regime

Table 4 lists the observed and simulated monthly runoff during the post-impact period. The number in bold indicates that the IHA value is significantly different compared to the observed and simulated values during the post-impact period at the 95% confidence level. Twenty-eight out of the 32 IHA metrics at the Zhangping (upper North River) and Punan (lower North River) stations experienced consistent decreased or increased changes, and the other 4 metrics exhibited no obvious changes for both stations, indicating that the Zhangping and Punan stations in North River had similar change patterns in IHA metrics. To compare the change pattern differences in the North and West River, the Zhangping (upper North River) and Punan (lower North River) stations were considered as one group called North River stations and Zhengdian station was called West River station. We assumed that a significant change in one IHA metric at any of the Zhangping and Punan stations in North River was considered to be a significant IHA metric change for the North River.

The changes in monthly runoff, rise rate, high pulse count, fall rate and number of reversals exhibit consistent patterns among the three stations, as shown in Table 4. The average monthly runoff in most months exhibited a nonsignificant difference. The rise rate and fall rate decreased dramatically, while the number of reversals increased dramatically. The high pulse counts at the North River and West River stations all decreased.

Most of the IHA metrics showed different patterns at the two river stations. The different patterns can be categorized into two types. 1) Both the North River and West River stations exhibit significant changes but have different change directions (e.g., one is positive and one is negative); 2) one river station changes significantly while the

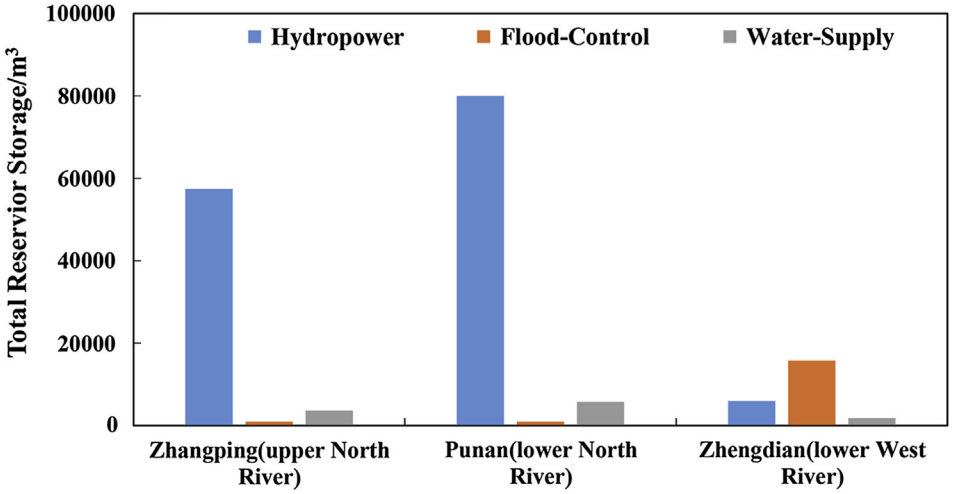

Fig. 6. Reservoir capacities of hydropower, flood-control and water-supply reservoirs in the drainage areas of Zhangping (upper North River), Punan (lower North River) and Zhengdian (lower West River) stations in Jiulong River basin by the end of 2011.

other one changes nonsignificantly.

The 3-day and 7-day minimum values and the low pulse count belonged to the first category. Specifically, the 3-day and 7-day minimums at the North River stations decreased significantly with relative changes below −20%, while those at the West River stations increased significantly. The low pulse counts at the North River stations significantly increased with an average relative change of 43.2%, while those at the West River stations decreased with a relative change of −43.8%.

The 30-day maximum value, base flow index, date of minimum flow, high pulse duration and low pulse duration belonged to the second category. At the West River station, the 30-day maximum value and date of minimum flow exhibited significant decreases, while the base flow index and high pulse duration increased significantly. However, these indicators did not exhibit significant changes at the North River stations. In contrast, the North River stations experienced significant changes in low pulse duration, while the West River stations exhibited no obvious changes.

Table 4
IHA results calculated by proposed framework at Zhangping (upper North River), Punan (lower North River) and Zhengdian (lower West River) stations.

IHA metrics	Post-impact period (1976–2014) Zhangping(upper North River)			Post-impact period (1976–2014) Punan(lower North River)			Post-impact period (1973–2014) Zhengdian(lower West River)		
	Obs	Sim	(Obs-Sim)/Obs (%)	Obs	Sim	(Obs-Sim)/Obs (%)	Obs	Sim	(Obs-Sim)/Obs (%)
January	52.8	52.5	0.5	91.5	95.4	−4.3	48.4	47.9	1.1
February	82.4	90.9	−10.3	138.5	161.3	−16.4	57.8	64.0	−10.6
March	153.7	177.9	−15.7	259.8	296.8	−14.2	83.6	95.2	−13.8
April	202.9	217.6	−7.2	338.7	356.7	−5.3	123.5	130.9	−5.9
May	258.9	307.6	−18.8	429.3	506.3	−17.9	164.9	182.8	−10.8
June	327.4	351.9	−7.5	579.1	603.2	−4.1	231.2	234.8	−1.6
July	162.7	153.5	5.7	321.6	310.1	3.6	181.0	187.3	−3.5
August	178.7	184.3	−3.1	362.6	366.8	−1.2	206.7	213.1	−3.1
September	128.8	144.9	−12.5	279.2	301.7	−8.1	190.7	196.6	−3.1
October	75.8	83.2	−9.7	150.9	166.6	−10.4	98.0	99.5	−1.6
November	57.8	65.8	−13.8	109.7	128.6	−17.3	70.6	72.9	−3.2
December	51.4	54.7	−6.5	93.2	105.8	−13.6	53.8	54.0	−0.4
1-day min	24.5	28.1	−14.5	42.2	57.5	**−36.2**	23.5	19.6	16.4
3-day min	26.5	28.4	−7.0	47.7	59.1	**−23.7**	24.8	20.0	**19.2**
7-day min	28.9	29.1	−0.6	53.2	61.6	**−15.8**	26.7	20.8	**22.0**
30-day min	37.4	35.3	5.6	67.3	74.3	−10.4	34.3	30.9	10.0
90-day min	56.1	57.4	−2.3	105.1	119.9	−14.1	50.7	51.9	−2.4
1-day max	1558.3	1755.4	−12.6	2687.2	2859.8	−6.4	1485.7	1825.7	−22.9
3-day max	1103.5	1146.7	−3.9	1946.2	2024.4	−4.0	1016.1	1147.7	−13.0
7−day max	771.0	794.1	−3.0	1348.2	1413.4	−4.8	681.8	787.7	−15.5
30-day max	457.4	489.0	−6.9	785.5	831.8	−5.9	359.3	396.8	**−10.4**
90-day max	303.8	329.6	−8.5	537.6	567.2	−5.5	246.6	259.3	−5.1
Base flow index	0.21	0.20	3.3	0.21	0.21	−3.0	0.22	0.15	**30.4**
Date of max	156.2	156.8	−0.4	170.6	170.0	0.4	207.9	213.3	−2.6
Date of min	137.7	133.3	3.2	114.8	130.0	−13.2	104.9	133.8	**−27.5**
Low pulse count	8.5	4.7	**44.7**	8.8	5.1	**41.7**	6.1	8.8	**−43.8**
Low pulse duration	8.1	16.0	**−96.1**	9.9	12.6	−27.3	7.8	13.4	−72.6
High pulse count	13.6	14.9	**−9.6**	13.0	14.0	−8.3	14.3	17.6	**−22.7**
High pulse duration	8.0	7.6	4.5	8.2	7.9	3.6	8.0	6.2	**22.8**
Rise rate	59.7	100.0	**−67.5**	99.2	143.7	**−44.8**	56.1	79.5	**−41.9**
Fall rate	35.4	41.6	**−17.5**	59.6	63.6	−6.7	29.5	36.3	**−23.0**
Number of reversals	158.6	127.1	**19.8**	149.7	115.8	**22.6**	138.5	123.4	**10.9**

Note: The number in bold means the parameter is significant at 95% confidence level using Mann-Whitney *U* test

5. Discussion

5.1. Comparison of the framework with the previously common method

Although the daily discharge simulations at the downstream west river station were still considered to be good (Moriasi et al., 2007), they were slightly worse compared to the north river stations. Before 1972 (the end of the validation period), the total reservoir storage were 33.31, 222.61 m^3 in the drainage area of Zhangping and Punan (North River) stations, respectively. The total reservoir storage the drainage area of Zhengdian (lower West River) station was 877.09 m^3, which is much larger than that of the North River stations. Therefore, the observed discharge at Zhengdian (lower West River) station during the calibration and validation period may deviate from the natural runoff. On the other hand, the model simulates the natural runoff. The slightly worse model simulations at the Zhengdian (lower West River) station may be caused by the deviation of observed runoff rather than the model limitations.

The relative change between simulated IHA results in Table S2 during the pre-impact and post-impact period represents the flow alteration caused by climate change from pre-impact period to post-impact period. It can be seen that the climate change from pre-impact period and post-impact period was demonstrated to have influences on flow regime such as monthly runoff during March and April, the multi minimum values, low pulse count and high pulse count. Table 5 lists the IHA for the three stations using the previously common method. The relative change calculated by the previously common method ($(Obs_{post} - Obs_{pre})/Obs_{pre}$ in Table 5) was compared to those calculated by the proposed framework ((Obs-Sim)/Obs in Table 4). Most of the IHA metrics calculated by the proposed framework had consistent statistical significance with those calculated by the previously common method. However, the monthly runoff data exhibited no clear change in the proposed framework, while the previously common method indicated increased monthly runoff, such as during March, at three stations and increased monthly runoff during 5 other months at the Zhengdian (lower West River) station. Moreover, the decreased multi-minimum values calculated by the proposed framework at the Punan (lower North River) station were not detected by the previously common method. The previously common method did not separate the impacts of climate change and dam construction on flow regime, which can mislead the estimations of the patterns of monthly runoff and multi-minimum values (Magilligan and Nislow, 2005; Zhao et al., 2012). As the minimum flow has played an important role in maintaining the normal functioning of the ecosystem (Rolls et al., 2012), it is necessary to use the framework instead of the previously common method to quantify the flow regime alteration induced by dams.

5.2. Dam-induced hydrological alterations: Comparison of hydropower and flood-control reservoirs

In the Jiulong River basin, the North River was dominated by hydropower reservoirs, while the West River was dominated by flood-control reservoirs according to the reservoir capacities (Fig. 6). The dominated reservoir type of river was determined by the type of reservoir that has the largest storage capacities. Zhang et al. (2015) stated that the hydropower facilities in the Jiulong River were small-scale (< 50 MW) dams. Irrespective of the dominant reservoirs in the North and West River, changes in monthly runoff, high pulse count, rise and fall rate and number of reversals were consistent between the North River and West River. The monthly runoff exhibited a nonsignificant difference. The high pulse count, rise rate and fall rate decreased while the number of reversals increased. Our results confirm the conclusions

Table 5
IHA results calculated by previous common method at Zhangping (upper North River), Punan (lower North River) and Zhengdian (lower West River) stations.

IHA metrics	Zhangping(upper North River)			Punan (lower North River)			Zhengdian (lower West River)		
	Obs_{pre}	Obs_{post}	$(Obs_{post}- Obs_{pre})/Obs_{pre}$ (%)	Obs_{pre}	Obs_{post}	$(Obs_{post}- Obs_{pre})/Obs_{pre}$ (%)	Obs_{pre}	Obs_{post}	$(Obs_{post}- Obs_{pre})/Obs_{pre}$ (%)
January	53.6	52.8	−1.5	97.6	91.5	−6.2	39.8	48.4	**21.6**
February	62.9	82.4	31.0	115.3	138.5	20.1	41.2	57.8	40.5
March	98.7	153.7	**55.7**	169.6	259.8	**53.2**	46.8	83.6	**78.7**
April	147.4	202.9	37.7	250.0	338.7	35.5	63.2	123.5	**95.6**
May	289.5	258.9	−10.6	460.1	429.3	−6.7	104.3	164.9	**58.1**
June	398.0	327.4	−17.7	683.9	579.1	−15.3	247.8	231.2	−6.7
July	173.8	162.7	−6.3	349.2	321.6	−7.9	189.2	181.0	−4.4
August	162.2	178.7	10.2	325.3	362.6	11.5	173.5	206.7	19.1
September	119.8	128.8	7.5	243.3	279.2	14.7	141.6	190.7	34.7
October	94.7	75.8	−19.9	185.3	150.9	−18.6	76.0	98.0	29.0
November	60.5	57.8	−4.5	116.9	109.7	−6.2	49.8	70.6	**41.7**
December	50.0	51.4	2.7	97.3	93.2	−4.2	41.8	53.8	**28.7**
1-day min	25.3	24.5	−3.1	50.6	42.2	−16.7	14.7	23.5	**59.7**
3-day min	25.7	26.5	3.2	51.9	47.7	−8.1	14.9	24.8	**66.1**
7-day min	27.3	28.9	5.7	54.5	53.2	−2.4	16.1	26.7	**66.2**
30-day min	35.7	37.4	4.7	69.6	67.3	−3.3	24.2	34.3	**41.5**
90-day min	54.3	56.1	3.5	102.8	105.1	2.2	36.2	50.7	**39.8**
1-day max	1906.2	1558.3	−18.2	3029.2	2687.2	−11.3	1479.6	1485.7	0.4
3-day max	1319.6	1103.5	−16.4	2147.4	1946.2	−9.4	936.7	1016.1	8.5
7-day max	931.9	771.0	−17.3	1526.4	1348.2	−11.7	613.0	681.8	11.2
30-day max	523.5	457.4	−12.6	871.8	785.5	−9.9	359.1	359.3	0.0
90-day max	318.3	303.8	−4.5	553.6	537.6	−2.9	222.9	246.6	10.7
Base flow index	0.2	0.2	5.1	0.2	0.2	−2.7	0.2	0.2	37.6
Date of max	176.8	156.2	−11.7	184.5	170.6	−7.5	207.2	207.9	0.4
Date of min	112.2	137.7	22.8	116.2	114.8	−1.2	123.2	104.9	−14.9
Low pulse count	6.8	8.5	23.7	6.8	8.8	28.3	11.5	6.1	**−46.8**
Low pulse duration	11.8	8.1	**−30.9**	11.3	9.9	−12.4	10.8	7.8	−27.8
High pulse count	14.5	13.6	−6.7	13.0	13.0	−0.2	14.6	14.3	-2.0
High pulse duration	6.2	8.0	**29.7**	6.7	8.2	23.2	5.3	8.0	**51.4**
Rise rate	88.3	59.7	**−32.4**	132.8	99.2	**−25.3**	63.7	56.1	−12.0
Fall rate	41.1	35.4	−13.7	62.5	59.6	−4.6	29.9	29.5	−1.3
Number of reversals	131.4	158.6	**20.7**	117.2	149.7	**27.7**	121.3	138.5	14.2

Note: The number in bold means the parameter is significant at 95% confidence level using Mann-Whitney *U* test.

of a previous study by Magilligan and Nislow (2005), who found that the number of reversals was increased by either hydropower or flood-control reservoirs. Changes in monthly runoff is in contrast to the results found for large dams, which reduced the streamflow during wet seasons and increased the streamflow during dry seasons (Li et al., 2017; Gao et al., 2012).

One large difference between the hydropower-dominated North River and the flood-control-dominated West River was associated with the magnitude of annual extreme streamflow. Increased minimum flow and decreased maximum flow in the West River are associated with the operation of large reservoir reserves. The large reservoirs can reduce the maximum flow significantly for providing flood suppression (Graf, 2006; Gao et al., 2012). In addition to preventing flood, the large reservoirs also need to release water to downstream users during dry seasons, which results in the increased minimum flow (Li et al., 2017; Räsänen et al., 2017). With respect to the hydropower-dominated North River, the decreased minimum flow was induced by hydropower generation, in which the small reservoir was designed for only power generation and needed to generate as much electricity as possible, and this reservoir may even store water to reach a sufficient head before generating electricity during dry seasons (Richter et al., 1996; Deitch et al., 2013; Li et al., 2017; Timpe and Kaplan, 2017). The lack of an obvious change in the maximum flow in the North River may be the result of the fact that small dams do not reduce high flows (Kibler and Tullos, 2013; Deitch et al., 2013).

The low pulse dynamics represented another different change pattern. The significantly decreased low pulse count in the West River indicated that the flood-control reservoir caused the reduction of the low pulse. This finding fits the commonly held belief that impoundment of flood-control reservoirs leads to increased minimum flows (Graf, 2006; Gao et al., 2012).

5.3. The possible impacts of hydrological alterations on river ecology

Our study demonstrated that both rivers exhibited consistent changes in the rise rate, high pulse count, fall rate and number of reversals. These changes may trap aquatic organisms in floodplain lakes and strand terrestrial organisms on floodplain islands (Timpe and Kaplan, 2017). The decreased high pulse count also reduced hydrological connectivity, which prevents exchange of matter, energy and organisms between floodplains and river systems, which should reduce the spawning area and recruitment success of river fish and lead to a decline in the richness and abundance of waterbird species and wetland vegetation through habitat fragmentation (Hu et al., 2008).

Changes in low-flow and high-flow magnitude showed different patterns in the North River and West River. The low-flow value decreased in the North River but increased in the West River. In the North River, the decreased low-flow magnitude contributed to a decrease in the water velocity, which directly led to accelerated channel bed sedimentation and aggravated the effects of water pollution, resulting in many concomitant biological changes (Smakhtin, 2001). During the dry period, the deterioration of the water quality, such as low oxygen contents and high levels of nutrients that are associated with decreasing low flow, can drive the production of phytoplankton and cyanobacteria, thereby contributing to significant and widespread occurrences of phytoplankton blooms associated with eutrophication (Vliet and Zwolsman, 2008; Bilotta and Brazier, 2008). The high flow value exhibited no obvious changes in the North River, but it decreased in the West River. Zhao et al. (2015) demonstrated that the sediment carried by high flow events was the main source of sediment in the Jiulong River estuary. Therefore, the decreased high flow in the West River may reduce the sedimentation in the Jiulong River estuary and change the high flow structure and morphology of the stream channel (Yang et al., 2012).

The low pulse and high pulse dynamics showed another different pattern in the North River and West River. The low pulse count increased in the North River and decreased in the West River. The increasing number of low pulses in the West River suggests that the richness of plant and animal species that are unable to tolerate or persist would decline, and the reduced number of low pulses in the North River support a greater proportion of plant and animal species with life-history traits that are unsuited to survival under low-flow conditions (Rolls et al., 2012). Either increased or decreased low pulse count influences soil moisture and anaerobic stress for plants and the availability of floodplain habitats for aquatic organisms (Graf, 2006). Therefore, maintaining a natural low pulse count is beneficial to aquatic system health, and a natural low pulse count at the downstream at least can be maintained possibly by operation of the last one (locates on the lower reach) of cascade dams.

The high pulse duration also exhibited no clear change in the North River but increased in the West River. The increased high pulse duration in the West River may lead to excessive hydrological connectivity, which is also expected to reduce habitat heterogeneity, with concomitant declines in biodiversity (Ward et al., 2010). In the North River, decreased high pulse counts and the lack of changes in the high pulse duration reduced the connectivity between floodplains and river systems, which was associated with declines in biodiversity. In the West River, increased high pulse duration and decreased high pulse count may offset the influence of each other on hydrological connectivity, which is beneficial to maintaining the balance of nutrient and organic matter exchanges between rivers and floodplains.

6. Conclusions

According to the results of this study, the following conclusions can be drawn.

(1) A framework that combined a hydrological model and the post bias correction method was proposed to investigate the effects of dam construction on IHA. The hydrological model (GBHM) used in this study can adequately reproduce the temporal variability of the streamflow in the Jiulong River basin. Considering the uncertainty of the IHA simulation, a post bias correction for the simulated IHA was accomplished by using the quantile mapping method. Compared to the previously common method that did not separate the impacts of climate change and dam construction on flow regime, the framework can effectively avoid the misleading of the change pattern of monthly runoff and multi-minimum values.
(2) Reservoir storages in the North River are built primarily for hydropower, while those in the West River are primarily used for flood control. Irrespective of the dominant reservoir type, the generally consistent change patterns of both rivers were as follows: the monthly river discharge exhibited no obvious change, the rise and fall rate decreased dramatically, the number of reversals increased significantly, and the high pulse count decreased.
(3) In the West River, the low-flow-related indicators, such as the base flow index and multi-day minimum flow, exhibited significant increases, while the multi-day maximum values exhibited significant decreases. In the North River, the multi-day minimum values decreased, and the maximum values exhibited no obvious change. With respect to the pulse dynamics, the low pulse count in the West River decreased with no clear change in the low pulse duration, while the low pulse count in the North River increased with a shorter low pulse duration. The high pulse duration increased in only the West River and exhibited no obvious change in the North River.

Our study implies that the minimum ecological water demand should be considered not only in the large reservoirs operation, but also in the operation of small hydropower reservoirs.

Acknowledgement

This work is financially supported by the National Natural Science Foundation of China (project Nos. 41661144031, 51679120).

Appendix A. Supplementary data

Supplementary data to this article can be found online at https://doi.org/10.1016/j.jhydrol.2018.10.034.

References

Arthington, A.H., Bunn, S.E., Poff, N.L., Naiman, R.J., 2006. The challenge of providing environmental flow rules to sustain river ecosystems. Ecol. Appl. 16 (4), 1311–1318.
Bilotta, G.S., Brazier, R.E., 2008. Understanding the influence of suspended solids on water quality and aquatic biota. Water Res. 42 (12), 2849–2861.
Boé, J., Terray, L., Habets, F., Martin, E., 2007. Statistical and dynamical downscaling of the Seine basin climate for hydro-meteorological studies. Int. J. Climatol. 27, 1643–1655. https://doi.org/10.1002/joc.1602.
Castello, L., Macedo, M.N., 2016. Large-scale degradation of Amazonian freshwater ecosystems. Glob. Change Biol. 22 (3), 990.
Dai, Y., et al., 2013. Development of a China dataset of soil hydraulic parameters using pedotransfer functions for land surface modeling. J. Hydrometeorol. 14 (3), 869–887.
Deitch, M.J., Merenlender, A.M., Feirer, S., 2013. Cumulative effects of small reservoirs on streamflow in northern coastal california catchments. Water Resour. Manage. 27 (15), 5101–5118.
Gao, B., Qin, Y., Wang, Y., Yang, D., Zheng, Y., 2016. Modeling ecohydrological processes and spatial patterns in the upper heihe basin in china. Forests 7 (1), 10.
Gao, B., Yang, D., Zhao, T., Yang, H., 2012. Changes in the eco-flow metrics of the Upper Yangtze River from 1961 to 2008. J. Hydrol. 30–38 448-449(s 448–449).
Gao, Y.X., Vogel, R.M., Kroll, C.N., Poff, N.L., Olden, J.D., 2009. Development of representative indicators of hydrologic alteration. J. Hydrol. 374 (1), 136–147.
Graf, W.L., 2006. Downstream hydrologic and geomorphic effects of large dams on American rivers. Geomorphology 79 (3), 336–360.
Gupta, H.V., Sorooshian, S., Yapo, P.O., 1999. Status of automatic calibration for hydrologic models: comparison with multilevel expert calibration. J. Hydrol. Eng. 4 (2), 135–143.
Hashino, T., Bradley, A.A., Schwartz, S.S., 2007. Evaluation of bias-correction methods for ensemble streamflow volume forecasts. Hydrol. Earth Syst. Sci. Discuss. 11 (2), 939–950.
Hu, W.W., Wang, G.X., Deng, W., Li, S.N., 2008. The influence of dams on ecohydrological conditions in the Huaihe River basin China. Ecol. Eng. 33 (3–4), 233–241.
Jarvis, A., Reuter, H.I., Nelson, A., Guevara, E., 2008. Hole-filled Seamless SRTM Data V4 Tech. rep. International Centre for Tropical Agriculture (CIAT).
Kibler, K.M., Tullos, D.D., 2013. Cumulative biophysical impact of small and large hydropower development in Nu River, China. Water Resour. Res. 49 (6), 3104–3118.
Kondolf, G.M., Rubin, Z.K., Minear, J.T., 2014. Dams on the Mekong: cumulative sediment starvation. Water Resour. Res. 50 (6), 5158–5169.
Li, D., Long, D., Zhao, J., Lu, H., Hong, Y., 2017. Observed changes in flow regimes in the Mekong River basin. J. Hydrol. 551.
Li, J., Ma, L., 2009. Background paper: Chinese renewables status report.
Li, Z., Yang, D., Gao, B., Jiao, Y., Hong, Y., 2015. Multiscale hydrologic applications of the latest satellite precipitation products in the Yangtze River Basin using a distributed hydrologic model. J. Hydrometeorol. 16 (1), 407–426.
Ligon, F.K., Dietrich, W.E., Trush, W.J., 1995. Downstream ecological effect of dams.
Lytle, D.A., Poff, N.L., 2004. Adaptation to natural flow regimes. Trends Ecol. Evol. 19 (2), 94–100.
Ma, H., Yang, D., Tan, S.K., Gao, B., Hu, Q., 2010. Impact of climate variability and human activity on streamflow decrease in the Miyun Reservoir catchment. J. Hydrol. 389 (3), 317–324.
Magilligan, F.J., Nislow, K.H., 2005. Changes in hydrologic regime by dams. Geomorphology 71 (1), 61–78.
Maidment, D.R., et al., 1993. Handbook of Hydrology. McGraw-Hill, New York.
Miao, Q., Yang, D., Yang, H., Li, Z., 2016. Establishing a rainfall threshold for flash flood warnings in China's mountainous areas based on a distributed hydrological model. J. Hydrol. 541 (541), 371–386.
Moriasi, D.N., et al., 2007. Model evaluation guidelines for systematic quantification of accuracy in watershed simulations. Trans. ASABE 50 (3), 885–900.
Nachar, N., 2008. The mann-whitney U: a test for assessing whether two independent samples come from the same distribution. Tutor. Quant. Methods Psychol. 4 (1).
Naiman, R.J., Decamps, H., Pollock, M., 1993. The role of riparian corridors in maintaining regional biodiversity. Ecol. Appl. 3 (2), 209–212.
Nash, J.E., Sutcliffe, J.V., 1970. River flow forecasting through conceptual models: Part 1 A discussion of principles. J. Hydrol. 10 (3), 282–290.
New, M., Hulme, M., Jones, P., 2000. Representing twentieth-century space-time climate variability. part ii: development of 1901–96 monthly grids of terrestrial surface climate. J. Clim. 12 (12), 829–856.
Nislow, K.H., Magilligan, F.J., Fassnacht, H., Bechtel, D., Ruesink, A., 2002. Effects of dam impoundment on the flood regime of natural floodplain communities in the upper Connecticut River. J. Am. Water Resour. Assoc. 38 (6), 1533–1548.
Olden, J.D., Poff, N.L., 2003. Redundancy and the choice of hydrologic indices for characterizing streamflow regimes. River Res. Appl. 19 (2), 101–121.
Panofsky, H.A., Brier, G.W., 1968. Some applications of statistics to meteorology.
Pettitt, A.N., 1979. A non-parametric approach to the change-point problem. Appl. Statistics 28, 126–135.
Piani, C., Haerter, J.O., Coppola, E., 2010. Statistical bias correction for daily precipitation in regional climate models over Europe. Theor. Appl. Climatol. 99 (1–2), 187–192.
Poff, N.L., et al., 2010. The ecological limits of hydrologic alteration (ELOHA): a new framework for developing regional environmental flow standards. Freshw. Biol. 55 (1), 147–170.
Räsänen, T.A., et al., 2017. Observed river discharge changes due to hydropower operations in the Upper Mekong Basin. J. Hydrol. 545, 28–41.
Reichle, R.H., Koster, R.D., 2004. Bias reduction in short records of satellite soil moisture. Geophys. Res. Lett. 31 (19), 187–206.
Richter, B.D., Baumgartner, J.V., Powell, J., Braun, D.P., 1996. A method for assessing hydrologic alteration within ecosystems. Conserv. Biol. 10 (4), 1163–1174.
Rolls, R.J., Leigh, C., Sheldon, F., 2012. Mechanistic effects of low-flow hydrology on riverine ecosystems: ecological principles and consequences of alteration. Freshw. Sci. 31 (4), 1163–1186.
Ryo, M., Iwasaki, Y., Yoshimura, C., Saavedra, V.O.C., 2015. Evaluation of spatial pattern of altered flow regimes on a river network using a distributed hydrological model. PLoS One 10 (7), e0133833.
Schneider, C., Laizé, C.L.R., Acreman, M.C., Rke, M.F., 2013. How will climate change modify river flow regimes in Europe? Hydrol. Earth Syst. Sci. Discuss. 17 (1), 325–339.
Sellers, P.J., 1996. A revised land surface parameterization (SiB2) for atmospheric GCMs, Part II : the generation of global fields of terrestrial biophysical parameters from satellite data. J. Clim. 9 (4), 706–737.
Shen, Y., Zhao, P., Pan, Y., Yu, J., 2014. A high spatiotemporal gauge-satellite merged precipitation analysis over China. J. Geophys. Res. Atmos. 119 (6), 3063–3075.
Shrestha, R.R., Peters, D.L., Schnorbus, M.A., 2014. Evaluating the ability of a hydrologic model to replicate hydro-ecologically relevant indicators. Hydrol. Process. 28 (14), 4294–4310.
Smakhtin, V.U., 2001. Low flow hydrology: a review. J. Hydrol. 240 (3), 147–186.
Smakhtin, V.Y., Sami, K., Hughes, D.A., 1998. Evaluating the performance of a deterministic daily rainfall-runoff model in a low-flow context. Hydrol. Process. 12 (5), 797–812.
Thrasher, B., Maurer, E.P., Mckellar, C., Duffy, P.B., 2012. technical note: bias correcting climate model simulated daily temperature extremes with quantile mapping. Hydrol. Earth Syst. Sci. 16 (9), 3309–3314.
Timpe, K., Kaplan, D., 2017. The changing hydrology of a dammed Amazon. Sci. Adv. 3 (11), e1700611.
van Genuchten, M., 1980. A closed-form equation for predicting the hydraulic conductivity of unsaturated soil. Soil. Sci. Soc. Am. J. 44, 892–898.
Vliet, M.T.H.V., Zwolsman, J.J.G., 2008. Impact of summer droughts on the water quality of the Meuse river. J. Hydrol. 353 (1–2), 1–17.
Wang, W., Lu, H., Yang, D., 2016a. Modelling hydrologic processes in the Mekong River Basin using a distributed model driven by satellite precipitation and rain gauge observations. PLoS ONE 11 (3), e0152229.
Wang, Y., Rhoads, B.L., Wang, D., 2016b. Assessment of the flow regime alterations in the middle reach of the Yangtze River associated with dam construction: potential ecological implications. Hydrol. Process. 30 (21), 3949–3966.
Ward, J.V., Tockner, K., Schiemer, F., 2010. Biodiversity of floodplain river ecosystems: ecotones and connectivity1. River Res. Appl. 15 (1–3), 125–139.
Yang, D., Herath, S., Musiake, K., 1998. Development of a geomorphology-based hydrological model for large catchments. Proc. Hydraul. Eng. 42, 169–174.
Yang, D., Herath, S., Musiake, K., 2002. A hillslope-based hydrological model using catchment area and width functions. Hydrol. Sci. J. 47 (1), 49–65.
Yang, D., Musiake, K., 2003. A continental scale hydrological model using the distributed approach and its application to Asia. Hydrol. Process. 17 (14), 2855–2869.
Yang, D., Koike, T., Tanizawa, H., 2004. Application of a distributed hydrological model and weather radar observations for flood management in the upper Tone River of Japan. Hydrol. Process. 18 (16), 3119–3132.
Yang, Z., Yan, Y., Liu, Q., 2012. Assessment of the flow regime alterations in the Lower Yellow River, China. Ecol. Inform. 10 (7), 56–64.
Zhang, Q., Xiao, M., Liu, C.L., Singh, V.P., 2014. Reservoir-induced hydrological alterations and environmental flow variation in the East River, the Pearl River basin, China. Stoch. Env. Res. Risk Assess. 28 (8), 2119–2131.
Zhang, Q., Zhang, Z., Shi, P., Singh, V.P., Gu, X., 2018. Evaluation of ecological instream flow considering hydrological alterations in the Yellow River basin, China. Glob. Planet. Change 160.
Zhang, Z., Huang, J., Huang, Y., Hong, H., 2015. Streamflow variability response to climate change and cascade dams development in a coastal China watershed. Estuar. Coast. Shelf Sci. 166, 209–217.
Zhao, H.B., Zhang, Q.H., Ting, X.U., 2015. Numerical modeling of flow and sediment movement on Jiulongjiang Estuary harbor. J. Sediment Res.
Zhao, Q., et al., 2012. The effects of dam construction and precipitation variability on hydrologic alteration in the Lancang River Basin of southwest China. Stoch. Env. Res. Risk Assess. 26 (7), 993–1011.
Ziv, G., Baran, E., Nam, S., Rodríguezíturbe, I., Levin, S.A., 2012. Trading-off fish biodiversity, food security, and hydropower in the Mekong River Basin. Proc. Natl. Acad. Sci. U.S.A. 109 (15), 5609.